



Supplement of

Improved retrieval of land ice topography from CryoSat-2 data and its impact for volume-change estimation of the Greenland Ice Sheet

J. Nilsson et al.

Correspondence to: Johan Nilsson (johan.nilsson@jpl.nasa.gov)

The copyright of individual parts of the supplement might differ from the CC-BY 3.0 licence.

1 S1 – Phase filtering and ambiguity corrections

2 To determine the effects of the phase filtering and phase ambiguity corrections steps in the SIN-
3 processing on accuracy and precision, a case study was performed over Barnes Ice Cap,
4 Nunavut, Canada. The Barnes Ice Cap was chosen as there was an extensive IceBridge ATM
5 campaign flown there in 2011. The analysis was divided up into four parts. First, both
6 corrections were applied in the processing and compared to ATM elevations within 50 m of each
7 ATM point; second, the phase ambiguity correction was omitted; third, the phase filtering was
8 omitted; and fourth, both corrections were omitted.

9 The case study was carried out using five months of CryoSat-2 data between February
10 and June 2011. The number of months was selected to maximize the number of comparison
11 samples on this relatively small ice cap. From the statistical analysis (Table S1), we observed
12 that the phase-filtering step accounted for most of the improvement, followed by the phase
13 ambiguity correction.

14 S2 – Implementation and selection of surface-fit algorithm

15 For this study a point-by-point (PP) elevation changes estimation procedure was used to derive
16 elevation changes following the approach of Wouters et al. (2015). This solution produced
17 significantly better results than solving for the elevation change rate on a regular grid (RG), as
18 employed by McMillan et al. (2014). The two methods were contrasted by gridding the PP
19 estimated elevation changes onto a regular grid with 1 km resolution and comparing to RG-
20 derived changes of the same resolution. The quality of the solutions was then estimated by
21 comparing to ATM elevation changes over the same time period by means of bilinear
22 interpolation. This produced agreements of $0.09 \pm 0.13 \text{ m a}^{-1}$ and $0.14 \pm 0.21 \text{ m a}^{-1}$ for the PP
23 and RG methods respectively, producing a difference in RMSE of 36%. The PP method further
24 exhibited an 80% lower sensitivity to surface slope compared to the RG method.

25 The higher locality of the solution in the PP method allows for a locally- and globally-
26 higher SNR compared to the RG method. This is due to the fact that the PP method captures
27 the local underlying topography in the solution to a higher degree, making it less sensitive to
28 small-scale surface undulations. In comparison, the grid-based methods solve for the local
29 topography over the entire grid cell area (1 km in this case). Statistically, one might argue that
30 the PP approach has the potential to introduce spatial correlations into the solution; however,
31 studies of the correlation length between the two products compared to ATM elevation change
32 residuals, does not support this argument.

33 In conclusion, we recommend the use of the point-based solution method (PP) over the
34 grid-based methods (RG), as they provide better agreement with ATM-derived elevation
35 changes, despite the drawback of higher computational cost.

36

37 S3 – Validation of surface elevations

38 We used ATM data spanning four separate years of spring campaigns, largely in the month of
39 April. The estimated surface elevations from the CryoSat-2 mission for both the ESA L2 product
40 and our processing was compared using a search radius of 50 m around each ATM location.
41 The difference between the two measurements was computed as CryoSat-2 minus ATM-formed
42 elevation residuals. The residuals were then edited for outliers using an iterative 3-sigma filter,
43 which stopped once the difference in standard deviation was less than 2%. The results of the
44 surface validation procedure are provided in Tables S2 and S3 and are separated according to
45 their individual modes.

46 The quality of the four DEMs used in our study (Table S4) was estimated in
47 approximately the same manner as the individual point observations described above, although
48 bilinear interpolation was used instead to estimate the DEM surface elevation at each ATM
49 location. Statistics were then computed for each ATM campaign (Table S4).

50 S4 – Validation of surface elevation changes

51 Due to the different time periods used the elevation change errors were multiplied with their
52 individual time spans as elevation change errors should be proportional to the uncertainty in the
53 repeat elevation measurements divided by the time between acquisitions. For the surface-fit
54 method a search radius of 175 m was used which is similar resolution as the ATM elevation
55 changes of 250x250 m (Krabill, 2014a) (product IDHDT4.001). The surface-fit method produces
56 the largest number of validation samples for all time periods. Comparing these results with the
57 crossover method, which used the same search radius for the validation, we found a lower
58 number of validation samples due to the lower spatial coverage produced by this method,
59 further aggravated by the availability of only one time-period for the validation procedure and
60 spatial sampling.

61 S5 – Determination of correlation length using semi-variogram analysis

62 To determine the correlation length of the estimated surface elevation changes to compute the
63 error budget we computed semi-variograms for both the LRM and SIN-mode for both products,
64 as seen in Figure S1. The semi-variogram was estimated from the elevation change residuals
65 between CryoSat-2 derived elevation changes and ATM. To merge residuals estimated from
66 many different time periods (2011-2013, 2011-2014, 2012-2014) each residual dataset was
67 multiplied with its corresponding time span. The merged dataset was then used to compute the
68 overall semi-variogram, which is seen in Figure S1. As spatial patterns of elevation change are
69 variable (i.e. topography dependent) the semi-variogram was computed separately for the SIN
70 and LRM-mode. From the individual semi-variograms we estimate a correlation length for the
71 LRM data of ~75 km and for SIN ~100 km.

72

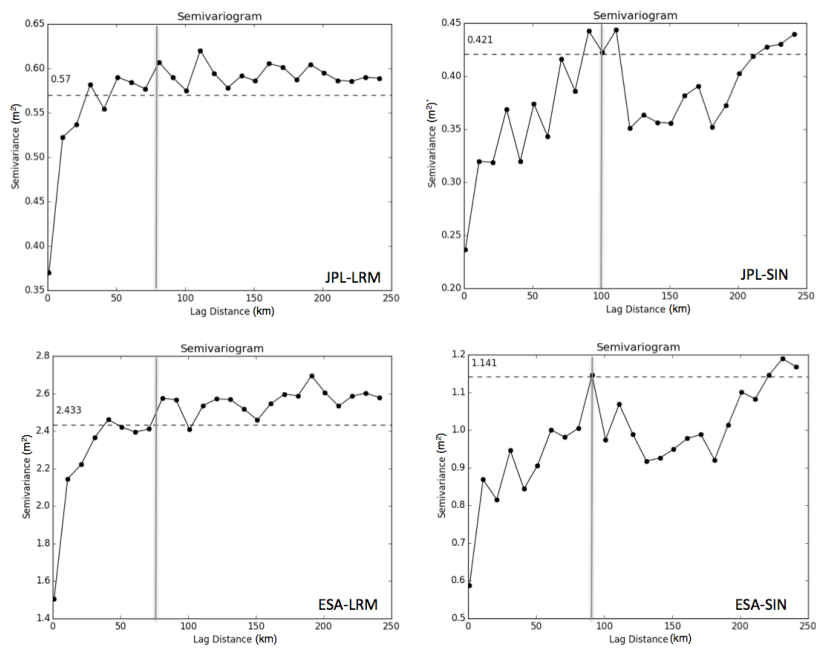
73

74 References

75 Krabill, William B.: IceBridge ATM L4 Surface Elevation Rate of Change [IDHDT4.001], Boulder,
76 Colorado USA, NASA DAAC at the National Snow and Ice Data Center,
77 <http://dx.doi.org/10.5067/BCW6CI3TXOCY>, 2014a (updated 2015).
78 Krabill, W. B.: IceBridge ATM L2 Icessn Elevation, Slope, and Roughness, Version 2 [ILATM2],
79 Boulder, Colorado USA, NASA National Snow and Ice Data Center Distributed Active
80 Archive Center, doi: <http://dx.doi.org/10.5067/CPRXXK3F39RV>, 2014b (updated 2016).
81 McMillan, M., Shepherd, A., Sundal, A., Briggs, K., Muir, A., Ridout, A., Hogg, A. and Wingham,
82 D.: Increased ice losses from Antarctica detected by CryoSat-2, *Geophys. Res. Lett.*,
83 41(11), 3899–3905, doi:10.1002/2014GL060111, 2014.
84 Wouters, B., Martin-Espanol, A., Helm, V., Flament, T., van Wessem, J. M., Ligtenberg, S. R.
85 M., van den Broeke, M. R. and Bamber, J. L.: Dynamic thinning of glaciers on the
86 Southern Antarctic Peninsula, *Science*, 348(6237), 899–903,
87 doi:10.1126/science.aaa5727, 2015.
88
89
90
91
92
93
94
95
96
97
98

99 **Figures**

100

101
102

103 *Figure S1: Semi-variograms estimated from CryoSat-2 and ATM residuals of elevation change*
 104 *from all three ATM data sets. The correlation length has been determined for each mode for*
 105 *both the JPL and ESA product, indicated by the grey vertical line. From these figures an*
 106 *approximate correlation length of 75 and 100 km was estimated for the LRM and SIN mode*
 107 *respectively.*

108 **Tables**

109 *Table S1: Effects on accuracy and precision when omitting SIN-processing steps over Barnes
 110 Ice Cap. Four test cases were completed to determine the influence of the different processing
 111 steps (phase-filtering and phase ambiguity correction) on the quality of the retrieved
 112 observations. Case-1 both the phase-filtering and ambiguity correction applied; Case-2 the
 113 ambiguity correction omitted; Case-3 the phase-filtering step omitted; Case-4 both steps have
 114 omitted. Statistics were calculated by comparing CryoSat-2 elevations with IceBridge ATM
 115 elevations. Here the Mean is the average of the residuals, SD is the standard deviation, RMSE
 116 the Root-Mean-Square-Error and N the number of observations.*

117

Case	Mean (m)	SD (m)	RMSE (m)	N
1	-0.36	0.61	0.71	282
2	-0.37	0.62	0.72	279
3	-0.42	0.70	0.82	241
4	-0.43	0.69	0.82	266

118

119 *Table S2: Validation of LRM surface elevations from CryoSat-2 compared to ATM surface
 120 elevations. The “Average” row shows the weighted mean-value (using the number of
 121 observations) of values. SD is the standard deviation, RMSE the Root-Mean-Square-Error and
 122 N the number of observations.*

123

LRM	Mean (m)	SD (m)	RMSE (m)	N
JPL - 2011	-0.18	0.30	0.35	2035
JPL - 2012	-0.06	0.60	0.60	2443
JPL - 2013	0.26	0.50	0.57	1054
JPL - 2014	0.09	0.35	0.36	3025
Average:	0.00	0.43	0.45	N/A
ESA - 2011	-1.36	0.91	1.64	2818
ESA - 2012	-1.45	1.17	1.87	2874
ESA - 2013	-0.56	0.71	0.90	1236
ESA - 2014	-0.70	0.72	1.01	3713
Average:	-1.06	0.89	1.40	N/A

124

125 *Table S3: Validation of SIN surface elevations from CryoSat-2 compared to ATM surface*
 126 *elevations, using CryoSat-2-data from the month of April. The “Average” row shows the*
 127 *weighted mean-value (using the number of observations) of values. SD is the standard*
 128 *deviation, RMSE the Root-Mean-Square-Error and N the number of observations.*

129

SIN	Mean (m)	SD (m)	RMSE (m)	N
JPL - 2011	-0.63	0.82	1.03	4475
JPL - 2012	-0.55	0.57	0.79	4010
JPL - 2013	-0.37	0.37	0.61	2309
JPL - 2014	-0.47	0.48	0.76	5504
Average:	-0.52	0.58	0.82	N/A
ESA - 2011	-0.95	1.20	1.53	4355
ESA - 2012	-1.19	1.31	0.91	4764
ESA - 2013	-0.76	0.95	1.22	2490
ESA - 2014	-0.87	0.73	0.96	5203
Average:	-0.90	1.05	1.13	N/A

130

131 *Table S4: Validation of four DEM’s using ATM surface elevations from four different campaigns*
 132 *over the Greenland Ice Sheet. The “Average” row shows the weighted mean-value (using the*
 133 *number of observations) of values. SD is the standard deviation, RMSE the Root-Mean-Square-*
 134 *Error and N the number of observations.*

135

DEM	Mean (m)	SD (m)	RMSE (m)	N
AWI - 2011	-2.03	6.48	6.79	4,216,153
AWI - 2012	-1.24	5.93	6.06	4,290,351
AWI - 2013	-0.32	6.74	6.75	2,690,046
AWI - 2014	-1.41	5.13	5.32	5,314,066
Average:	-1.35	5.95	6.12	N/A
GIMP - 2011	-1.44	7.89	8.02	4,481,612
GIMP - 2012	-1.35	7.25	7.38	4,427,566
GIMP - 2013	-0.22	7.40	7.40	2,764,105
GIMP - 2014	-1.15	6.56	6.66	5,541,920
Average:	-1.13	7.22	7.32	N/A
JPL - 2011	-1.27	6.77	6.89	4,336,066
JPL - 2012	-1.16	6.14	6.24	4,320,667
JPL - 2013	0.07	6.81	6.81	2,682,035
JPL - 2014	-0.79	5.85	5.90	5,443,766
Average:	-0.87	6.31	6.39	N/A
ESA - 2011	-3.48	6.75	7.59	4,321,714
ESA - 2012	-2.91	5.87	6.55	4,231,174
ESA - 2013	-2.17	6.80	7.14	2,667,683
ESA - 2014	-2.57	5.50	6.08	5,356,199
Average:	-2.83	6.13	6.76	N/A

136

137 *Table S5: Validation of SF-SIN surface elevation changes from CryoSat-2 compared to ATM*
 138 *surface elevation changes, using CryoSat-2-data from within a search radius of 175 m of the*
 139 *ATM-locations. The “Average” row shows the weighted mean-value (using the number of*
 140 *observations) of values SD is the standard deviation, RMSE the Root-Mean-Square-Error, N the*
 141 *number of observations and SE the residual slope error*

142

SF - SIN	Mean (m)	SD (m)	RMSE (m)	N
JPL – 2011-13	0.36	0.68	0.78	20,051
JPL – 2011-14	0.33	0.57	0.66	102,613
JPL – 2012-14	0.26	0.58	0.64	94,630
Average:	0.30	0.58	0.66	N/A
ESA – 2011-13	0.48	1.18	1.26	22,844
ESA – 2011-14	0.33	0.99	1.05	112,091
ESA – 2012-14	0.32	1.10	1.14	101,042
Average:	0.34	1.06	1.11	N/A

143

144 *Table S6: Validation of SF-LRM surface elevation changes from CryoSat-2 compared to ATM*
 145 *surface elevation changes, using CryoSat-2-data. The “Average” row shows the weighted mean-*
 146 *value (using the number of observations) of values. SD is the standard deviation, RMSE the*
 147 *Root-Mean-Square-Error and N the number of observations.*

148

SF - LRM	Mean (m)	SD (m)	RMSE (m)	N
JPL – 2011-13	0.32	0.56	0.64	6,639
JPL – 2011-14	0.18	0.69	0.69	14,643
JPL – 2012-14	-0.02	0.70	0.70	18,950
Average:	0.11	0.67	0.69	N/A
ESA – 2011-13	0.66	1.56	1.70	8,679
ESA – 2011-14	0.54	1.50	1.59	18,142
ESA – 2012-14	-0.20	1.50	1.50	19,846
Average:	0.25	1.51	1.57	N/A

149

150

151

152

153

154

155

156

157

158

159

160

161

162 *Table S7: Validation of XO crossover surface elevation changes from CryoSat-2 (2011-2014)*
 163 *compared to ATM surface elevation changes. SD is the standard deviation, RMSE the Root-*
 164 *Mean-Square-Error and N the number of observations.*

165

XO - LRM	Mean (m)	SD (m)	RMSE (m)	N
JPL	0.24	0.72	0.78	683
ESA	0.60	1.02	1.20	557
XO - SIN				
JPL	-0.06	1.26	1.26	12,075
ESA	-0.21	1.44	1.44	10,477

166